Quantification of plume-soil interaction and excavation due to the sky crane descent stage.

Jeffrey Vizcaino[1] and Manish Mehta[2]
NASA Marshal Space Flight Center, Huntsville, Al, 35811

The quantification of the particulate erosion that occurs as a result of a rocket exhaust plume impinging on soil during extraterrestrial landings is critical for future robotic and human lander mission design. The aerodynamic environment that results from the reflected plumes results in dust lifting, site alteration and saltation, all of which create a potentially erosive and contaminant heavy environment for the lander vehicle and any surrounding structures. The Mars Science Lab (MSL), weighing nearly one metric ton, required higher levels of thrust from its retro propulsive systems and an entirely new descent system to minimize these effects. In this work we seek to quantify plume soil interaction and its resultant soil erosion caused by the MSL's Sky Crane descent stage engines by performing three dimensional digital terrain and elevation mapping of the Curiosity rover's landing site.

Analysis of plume soil interaction altitude and time was performed by detailed examination of the Mars Descent Imager (MARDI) still frames and reconstructed inertial measurement unit (IMU) sensor data. Results show initial plume soil interaction from the Sky Crane's eight engines began at ground elevations greater than 60 meters and more than 25 seconds before the rovers' touchdown event. During this time, viscous shear erosion (VSE) was dominant typically resulting in dusting of the surface with flow propagating nearly parallel to the surface. As the vehicle descended and decreased to four powered engines plume-plume and plume soil interaction increased the overall erosion rate at the surface. Visibility was greatly reduced at a height of roughly 20 meters above the surface and fell to zero ground visibility shortly after. The deployment phase of the Sky Crane descent stage hovering at nearly six meters above the surface showed the greatest amount of erosion with several large particles of soil being kicked up, recirculated, and impacting the bottom of the rover chassis.

Image data obtained from MSL's navigation camera (NAVCAM) pairs on Sols 002, 003, and 016 were used to virtually recreate local surface topography and features around the rover by means of stereoscopic depth mapping. Images taken simultaneously by the left and right navigation cameras located on the rover's mast assembly spaced 42 centimeters were used to generate a three dimensional depth map from flat, two dimensional images of the same feature at slightly different angles. Image calibration with physical hardware on the rover and known terrain features were used to provide scaling information that accurately sizes features and regions of interest within the images. Digital terrain mapping analysis performed in this work describe the crater geometry (shape, radius, and depth), eroded volume, volumetric erosion rate, and estimated mass erosion rate of the Hepburn, Sleepy Dragon, Burnside, and Goulburn craters. Crater depths ranged from five to ten centimeters deep influencing an area as wide as two meters in some cases. The craters formed were highly asymmetrical and generally oblong primarily due to the underlying bedrock formations underneath the surface. Comparison with ground tests performed at the NASA AMES Planetary Aeolian Laboratory (PAL) by Mehta showed good agreement with volumetric erosion rates and crater sizes of large particle soil simulants, providing validation to Earth based ground tests of Martian regolith.

Nomenclature

D_e = Equivalent Engine diameter
X = Lateral ground plane direction
Y = Ground plane direction orthogonal to X direction

[1] Aerospace Engineer, Qualis Corporation - Jacobs ESSSA Group, Huntsville, Alabama 35806
[2] Aerothermal Engineer, MSFC EV33 Aerosciences Branch, AIAA Professional Member

Z = Altitude direction orthogonal to XY Plane

I. Introduction

Extraterrestrial lander vehicles employ the use of retro rockets to decrease their velocity when entering the touchdown phase of final descent. The use of retro rockets creates a high pressure bubble and zones of recirculation underneath the lander which can potentially kick up soil and dislodge small rocks. Brief interactions of the jets from three engines of the Viking lander with the Martian soil caused modest surface erosion during its landing however, the Phoenix landers' twelve engines with 2/3 total thrust of the Viking lander pulsating at 10Hz with an average impingement pressure of only 1/10 of the Earth's sea level pressure caused extensive erosion of the landing site and exposed subsurface ice under the lander over a radius between 75 and 85 cm from its centerline. The Phoenix inertial measurement unit (IMU) indicates that lift loss started when the spacecraft was approximately five meters above the surface, while descending at 2.6 m/s suggesting that the exhaust plume interacted with the soil for less than two seconds.

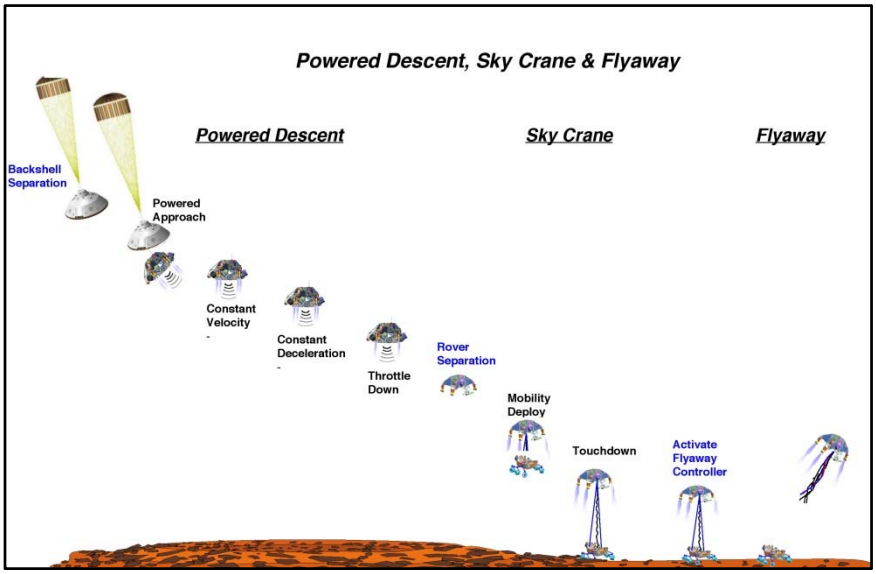

Figure 1: MSL Descent Phase. *The powered descent phase ends with the Sky Crane Maneuver in which the Curiosity Rover is lowered by cable while the descent state hovers several meters above the ground*

Extensive site-alteration can result in destabilization of the spacecraft during descent and possibly after lander touchdown which would ultimately lead to mission failure. The liberated particles have sufficient momentum to travel significant distances or potentially strike the landing vehicle with damaging force. Indeed this was the case with Surveyor III and the subsequent landing of the Apollo 12 lunar module. Despite the Lunar Excursion Module (LEM) landing roughly a 163 m away from the Surveyor vehicle and uphill along a crater rim, returned samples of the vehicle had shown evidence of sand blasting and pitting on exposed surfaces and even soil deposition inside some instruments. A study performed using NASA gas flow codes and mathematical analysis determined that the smallest particles could travel between 300-2000 m/s and some even exceeding 2.37 km/s, the escape velocity of the moon[1]. Analysis from Apollo landing footage suggests that the angle of particle ejection was approximately 1-3 degrees[1], with no atmosphere on the moon these energetic soil particles have the potential to travel several kilometers before settling, potentially striking nearby structures and future settlements.

The understanding and assessment of rocket plume-soil interaction environments is vital for human space flight missions. The thrust of the descent engines for these 30-50 metric ton landers will also need an order-of- magnitude larger sized propulsion systems. Comparatively, MSL's Curiosity was a one metric-ton rover and needed about 2800 lb_f of thrust for its final descent stage.

II. Plume-Soil Interaction Height

High resolution image captures from the Mars Descent Imager (MARDI), located on the front left side of the Curiosity rover facing down, were used to determine the height at which the plume was first observed to interact with the Martian regolith. Figure 2 shows a sequence of images detailing the start and termination of plume surface interactions. The altitudes shown are in the Sky Crane reference frame and thus a height of approximately 6 meters represents minimum height at which point the rover is gently lowered to the surface. In the figure, thrusters are shown to be interacting with the surface for approximately 25 seconds before the release and fly away maneuver which correlates to approximately 63 meters above the ground. Normalized to the equivalent engine nozzle diameter for each crater (1 engine with an exit diameter of 20 cm) yields an initial height of ~315 D_e and an engine cut off height of 30 D_e.

Figure 2: MARDI images taken during descent phase. *Correlated MARDI images with trajectory data shows rocket thruster – soil interaction occurs at roughly 63 meters above the surface at 25 seconds before touchdown. Significant erosion occurs within the last 15 seconds.*

Initial impingement of the surface results only in minor viscous shear erosion contributing little to formation of a crater. From a hazard perspective, these high velocity microscopic particles pose a threat to the nearby surroundings likely to cause sandblasting and deposition on unprotected surfaces. At 18 meters, roughly ten seconds

after initial plume impingement has occurred there is significant erosion occurring and much of the ground is obscured. At ten meters and below one can see that the surface is completely hidden by debris and ejecta material being recirculated underneath the vehicle. Previous observations by Mehta[2] have noted that significant erosion under similar conditions did not occur until the engine nozzles were roughly five to six meters above the soil surface. The Sky Crane descent stage with its larger engines roughly triples this height. At six meters altitude just before touchdown and fly away, there is zero visibility due to plume induced soil erosion.

Figure 3 below shows the trajectory of the Sky Crane system over its last 100 meters above ground before it performs the release and fly away maneuver. The eight descent engines are throttled down to four at approximately T- 21.1 seconds at an altitude of roughly 23 meters above the ground. Analysis of the vehicle's ground track shows that it moved approximately 40 cm in the X plane and 60 cm in the Y plane during its final 20 meters of descent. This data shows that the resultant craters formed were formed from continuous impingement and likely represent the maximum depth that could have formed. If there had been more lateral movement during the descent a shallow crater would likely have been formed albeit with a much wider area of influence due to less soil interaction time per region. The amount of lateral movement is unlikely to have resulted in significant widening of the crater though it is a possibility.

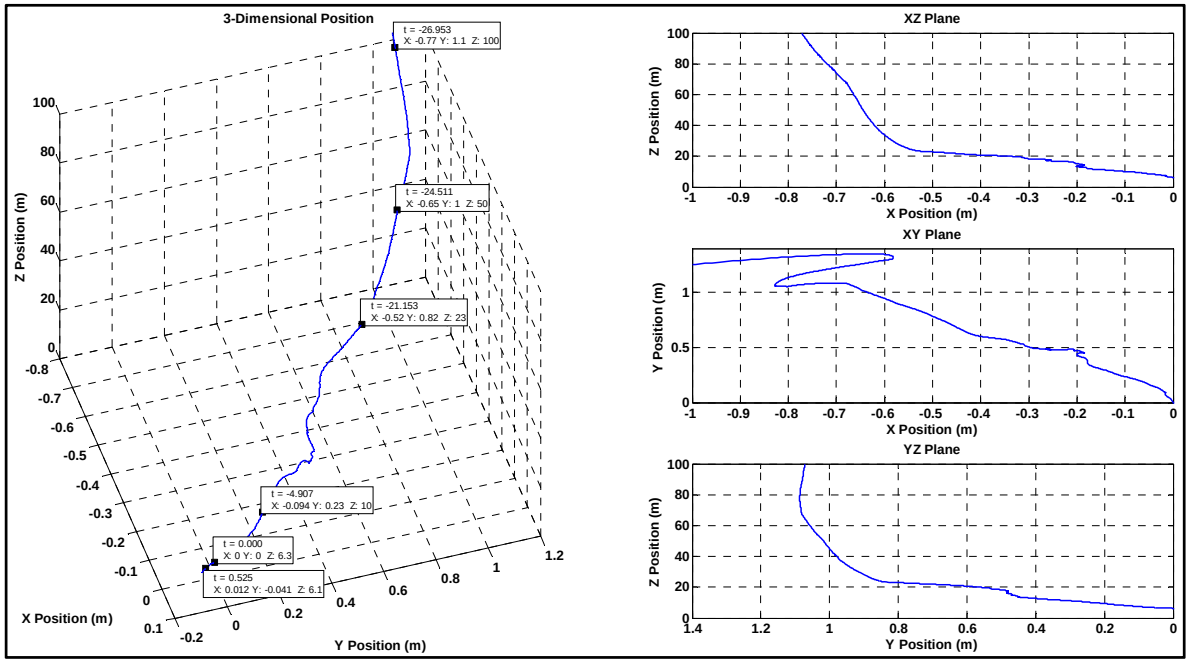

Figure 3: Ground Track of Descent Phase. *The last 100 meters of the descent phase show the ground tracks in the XYZ coordinate frame of the lander. Very little translation occurs in the final meters where soil interaction occurs.*

III. Image correlation and calibration

The Mars Science Lab rover uses a pair of left and right NAVCAMs (outlined in Figure 4) spaced 42.4 cm apart with an f/12 aperture and fixed focal length of 14.67 mm which produce a 45 x 45 degree field of view. Each camera has a one megapixel resolution (1024 pixels x 1024pixels) with 12 micron sized pixels and a focus range between 0.5 meters and infinity enabling high resolution, wide angle stereo pair image capture (shown in Figure 5).

Cardinal Systems' VrMapping® VrTwo software, used to perform analysis, requires that the stereoscopic images be calibrated with geometric scale information of objects and features in view. Normally this is done by the use of fiduciary scaling points, which have a known position and spacing relative to the camera's location. The Curiosity rover contains these points throughout its chassis but they were not in frame coincidentally with the exhaust craters during most of the imaging activities. The primary images used for reconstructing the exhaust craters were taken on Sol 016 of the MSL mission and are referenced in Table 1. During this time, the rover had performed a panning sweep consisting of five separate overlapping images near its landing site and are compiled Figure 6.

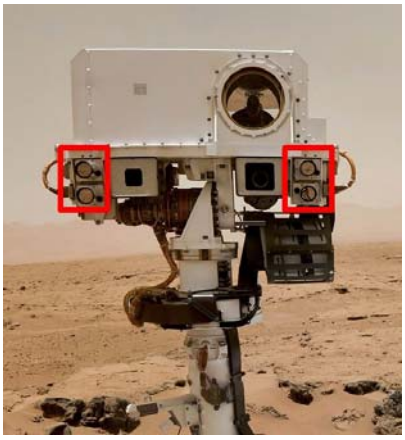

Figure 4: Left and Right stereo NAVCAMs.

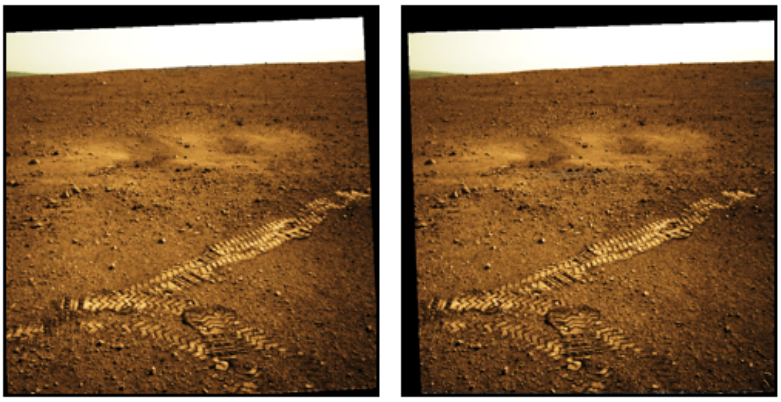

Figure 5: Left and Right NAVCAM images. *Simultaneously captured stereo pair images with crater geometry shown in the background.*

The two sets of craters shown in Figure 6 were found individually in separate frames. None of the images had rover hardware in view and thus no fiduciary scaling points. Several indirect scale references were left behind by the rover as it moved away from its landing site. Two sets of tire tracks and treads are shown in the stereo image pairs which were used as calibration features to compare against dimensions from MSL's flight hardware. The hardware values were extracted from an engineering CAD model of the Curiosity rover provided by NASA's Jet Propulsion Laboratory. Table 2 lists a summary of the features extracted from the stereo pairs.

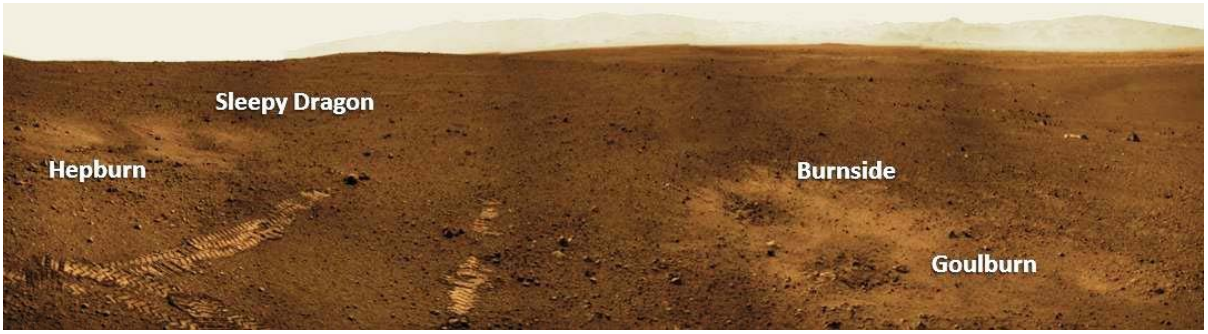

Figure 6: Landing Site Panoramic. *Two pairs of craters formed by the Sky Crane maneuver are visible in this composite panoramic.*

Table 1: MSL NAVCAM Images

Left NAVCAM	Right NAVCAM
NLA_398919509EDR_F0030078NCAM00300M1	NRA_398919509EDR_F0030078NCAM00300M1
NLA_398919544EDR_F0030078NCAM00300M1	NRA_398919544EDR_F0030078NCAM00300M1
NLA_398919572EDR_F0030078NCAM00300M1	NRA_398919572EDR_F0030078NCAM00300M1
NLA_398919607EDR_F0030078NCAM00300M1	NRA_398919607EDR_F0030078NCAM00300M1
NLA_398919642EDR_F0030078NCAM00300M1	NRA_398919642EDR_F0030078NCAM00300M1

As observed in Figure 7, some of the craters shown have no calibration features in its frame and partial craters in its frame. The images were taken in one panoramic sequence which allowed the VrMapping® software to perform an automatic feature detection routine that cross referenced the five individual images with each other and correlated points of similarity between all images. The degree of correlation can be seen by the green, yellow, and orange dots within the panoramic images shown in Figure 7. Each dot represents a recognized unique feature present in one, two, or three images respectively. Automated correlation across the five image pairs allows the program to use scaling data from one image and apply it across all other images.

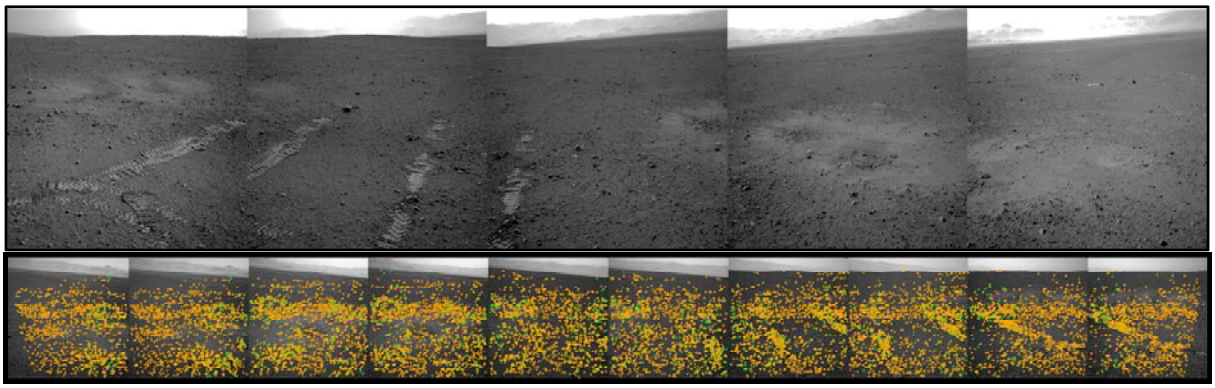

Figure 7: Image sequences for MSL surface reconstruction. *Several image sequences were combined from the left and right NAVCAMS were used to perform cross correlation of the images to provide scaling information for geometry present in individual frames.*

Table 2: Model Calibration Features

Feature	Feature Location Description	CAD Measurement (cm)	Average Mapped Measurement (cm)
1	Tire Width	39.5	40.6
2	Tread Spacing	5.3	5.38
3	Center Tread Length	10.5	10.1
4	Center Wheel Spacing	212.5	221
5	“JPL” Morse Code Spacing	3.40	3.48
6	“JPL” Morse Code Width	3.0 – 6.0	4.5*-6.76

*Not all of the Morse code indentations were present in mapped images

IV. Digital Elevation Mapping

The scaled and calibrated images were generated using the above data. A ground (XY) plane is defined by the user as a flat surface of level height. The images are presented as rotated and scaled stereo pairs, that when combined present the user with a depth field that allows him or her to distinguish edges of well-defined objects in the image. The user defines points on the image for features of interest (rocks, crater bounds, depressions, peaks, etc.) by adjusting the focus of three dimension image which has the effect of scaling the Z elevation above the ground XY plane. The relative coordinate locations are defined and calculated completely by the program.

A Digital elevation Map (DEM) is generated by defining points and break lines. Singular points define the local elevation of the surface and detail small features that can be sufficiently defined by triangular geometry such as pebbles and small dips. Break lines are used to define regions of sharp changes such as cliffs, large rocks, and steep walls.

A triangular mesh is generated when the region of interest is sufficiently defined by a network of points and break lines. A smoothing algorithm generates contours lines from the triangular mesh which is used to visually represent the final geometry.

Crater volume is determined by differencing the volume between an outer bounding region and the previously generated DEM. A bounding profile is manually defined by tracing the rim of the crater using a series of break lines then a planar fill surface is fitted across the closed profile. An underlying assumption is that the surface was initially flat before the plume-soil interaction event.

The coordinate system for the resultant map is defined relative to the camera field of view and its viewing plane. Depth measurements are taken relative to the rim around each individual crater rather than the ground plane.

Figure 9 and Figure 10 present digital maps of the four craters formed during landing, shown in Figure 6 and detailed in

Table 3. Qualitatively the Sleepy Dragon, Hepburn, and Burnside craters had the largest crater radius and depth eroded. The Goulburn crater had the shallowest and least extensive radii most likely due to the presence of large bedrock formations directly underneath the impingement area.

Visual inspection of the NAVCAM images showed that the Sleepy Dragon crater was relatively free of pebbles and other large debris after soil erosion, the Hepburn crater showed larger rocks deposited along the rim of its crater but was otherwise featureless. It is not clear if this was due to a sparsely populated terrain, more severe soil erosion, or the lack of subsurface bedrock like that found in the Burnside and Goulburn craters. Visual inspection of non-stereo images captured by the Curiosity's

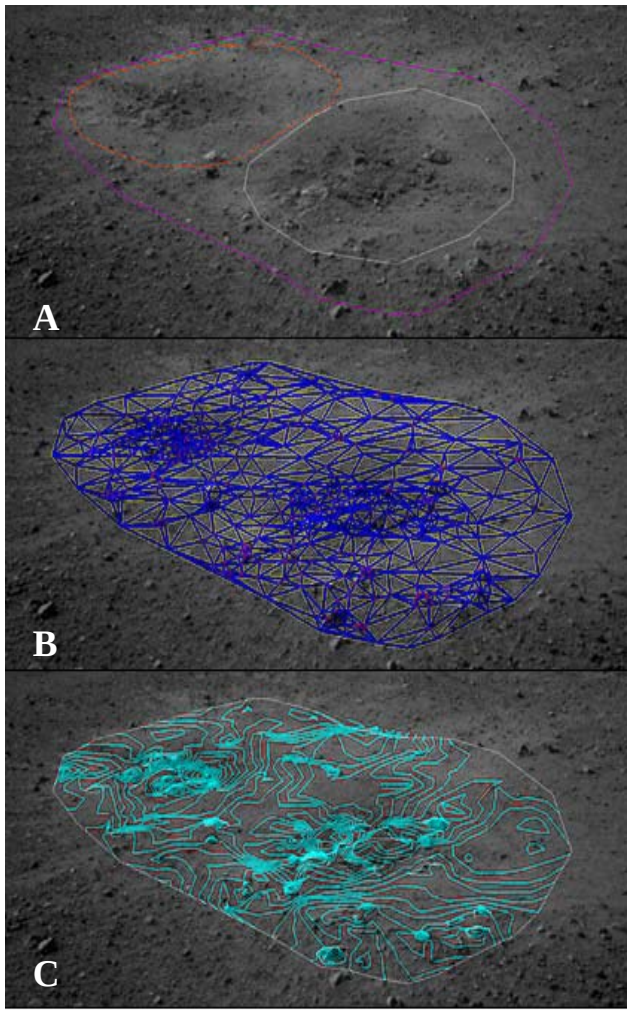

Figure 8: DEM Generation. *From top to bottom, mapping region selection (A), tessellation (B), contour smoothing (C) and 3D map generation (D).*

MASTCAM instrument of the same region seems to indicate that there was a slight ground slope near the region Hepburn crater and Sleepy Dragon craters which could have altered the erosion rates.

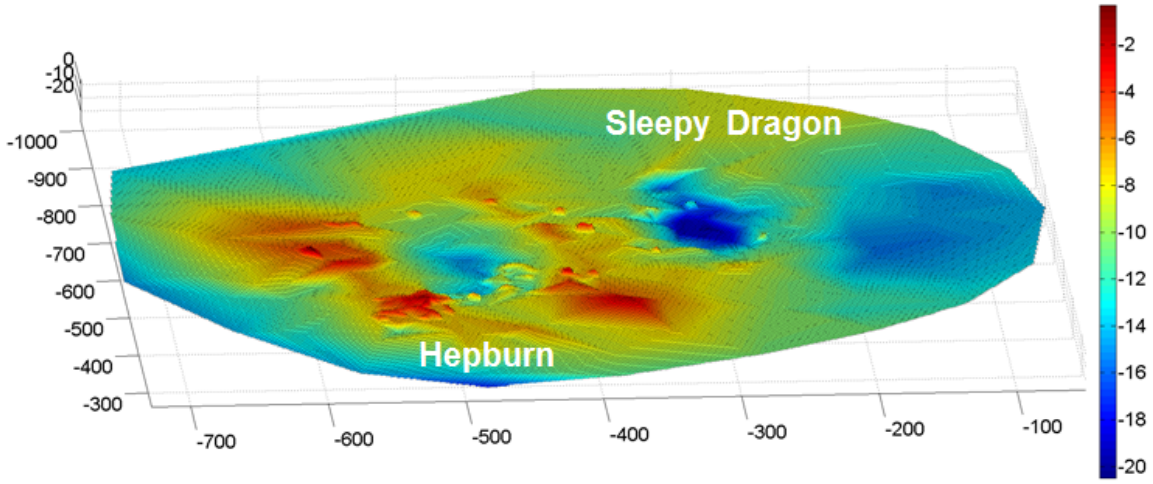

Figure 9: Hepburn and Sleepy Dragon crater features. Units shown in (cm), depth relative to ground plane.

The presence of subsurface bedrock formations beneath the layer of loose topsoil in the region of the Burnside and Goulburn craters prevented further plume induced erosion in a manner similar to what was observed from the Phoenix vehicle landed near the northern Martian pole. A solid water ice layer was exposed a few centimeters below the surface when the pulsed thrusters made contact with the ground; experimental results showed that the presence of this layer inhibited soil penetration depth though it resulted in approximately the same crater radius[3]. The rocket exhaust plumes are no longer able to 'dig' through the soil and reverts back to shearing the top soil layers.

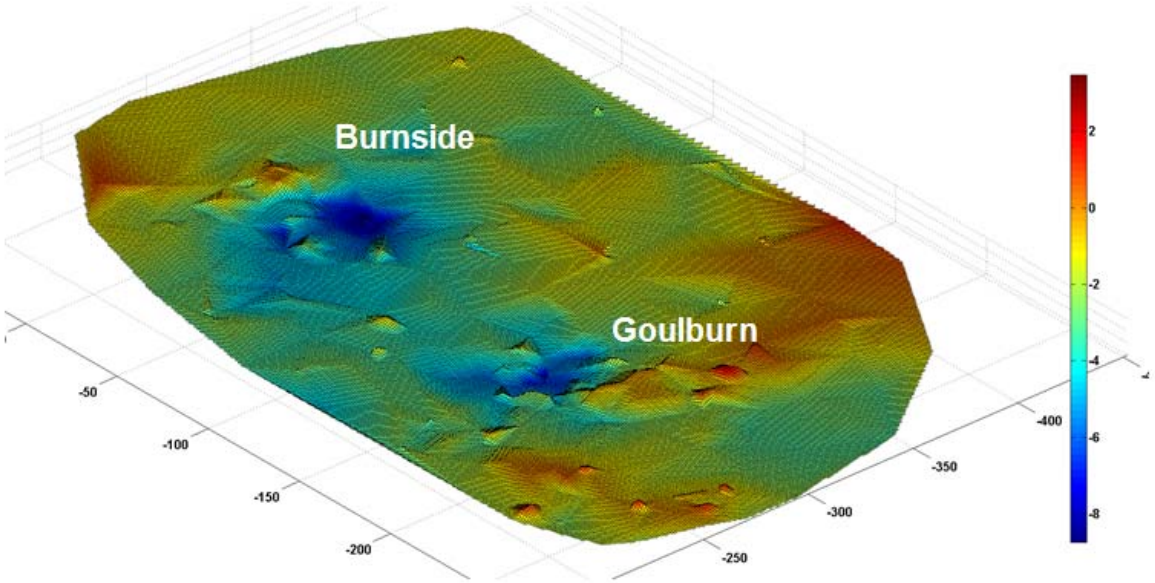

Figure 10: Burnside and Goulburn crater features. Units shown in (cm), depth relative to ground plane.

Table 3: Crater Properties

Crater	Name	Eroded Volume (m^3)	Maximum Depth (m)	Approximate Diameter (m)
1	Goulburn	0.011	0.067	1.330
2	Burnside	0.054	0.051	1.740
3	Hepburn	0.064	0.073	2.000
4	Sleepy Dragon	0.085	0.102	2.240

V. Erosion Rate

The volumetric erosion rates were estimated by utilizing the extracted volume data and descent time from the MARDI images. As noted previously, plume soil interaction and erosion occurs roughly 25 seconds before touchdown however this method of erosion, known as viscous shear (VSE), produces little volumetric erosion. The anticipated erosion method, bearing capacity failure (BCF), is far more severe with erosion rates that are generally an order of magnitude higher than that of VSE. If we estimate that BCF erosion occurs at 18 meters, the point in which we can no longer see the ground, the estimated total interaction time is on the order of 15 seconds.

The estimated volumetric erosion rates compare well when analyzed against experimental results from Metha[4]. With exception of the Goulburn crater, the craters fall into the upper region of estimated erosion rates dominated by coarse, large grained soils.

Table 4: Comparison of simulated erosion rates and those estimated from MSL Sky Crane descent stage[3]

Test	Test #	Soil Type	Volume (m^3)	Time (s)	Volumetric Erosion Rate (m^3/s)
MSL	8	Mars (Fine Sand)	3.29E-04	0.94	3.51E-04
MSL	7	Mars (Fine Sand)	4.91E-04	0.96	5.12E-04
MSL - Flight	**Goulburn**	**N/A**	**1.09E-02**	**15**	**7.27E-04**
MSL	2	Mars (Fine Sand)	5.86E-04	1.1	5.35E-04
MSL	23	Mars (Coarse)	9.51E-04	1	9.51E-04
MSL	13	Mars (Fine Sand)	1.07E-03	1	1.07E-03
MSL	21	Mars (Coarse)	1.11E-03	0.95	1.17E-03
MSL	6	Mars (Fine Sand)	1.10E-03	0.94	1.17E-03
MSL	16	Mars (Coarse)	1.44E-03	0.95	1.52E-03
MSL	5	Mars (Fine Sand)	1.65E-03	0.98	1.69E-03
MSL	12	Mars (Fine Sand)	1.97E-03	0.98	2.01E-03
MSL	18	Mars (Coarse)	1.64E-03	0.69	2.39E-03
MSL	20	Mars (Coarse)	2.92E-03	1	2.93E-03
MSL	4	Mars (Fine Sand)	2.35E-03	0.78	3.01E-03
MSL	15	Mars (Coarse)	3.85E-03	1	3.85E-03
MSL - Flight	**Burnside**	**N/A**	**5.38E-02**	**15**	**3.59E-03**
MSL - Flight	**Hepburn**	**N/A**	**6.36E-02**	**15**	**4.24E-03**
MSL - Flight	**Sleepy Dragon**	**N/A**	**8.47E-02**	**15**	**5.65E-03**
MSL	22	Mars (Coarse)	5.01E-03	0.89	5.65E-03
MSL	17	Mars (Coarse)	6.69E-03	0.96	6.98E-03
MSL	19	Mars (Coarse)	6.88E-03	0.97	7.09E-03
MSL	14	Mars (Coarse)	1.67E-02	0.97	1.72E-02

If we are to estimate the average bulk density of the soil in the region is approximately equal to that of coarse soil simulant we can obtain a total mass eroded in each crater, shown in Table 5.

Table 5: Estimated Eroded Mass from MSL Sky Cane Descent Stage

Test	Test #	Soil Type	Eroded Mass (m^3)
MSL - Flight	Goulburn	Mars (Coarse)	4.25
MSL - Flight	Burnside	Mars (Coarse)	21.0
MSL - Flight	Hepburn	Mars (Coarse)	24.8
MSL - Flight	Sleepy Dragon	Mars (Coarse)	33.0

VI. Conclusion

Erosion caused by the Sky Crane descent stage was identified and quantified. The MARDI camera allowed us to determine, for the first time, when plume-soil interaction began to occur which was found to be approximately 63 meters above the ground level. Soil erosion continuously increased and visibility decreased as the Sky Crane descends to its final altitude.

The data extraction methods employed to the MSL data were a value added benefit and was performed without a need to alter the vehicle or collaborate with mission planners during design phase. Scientists analyzing future human and robotic missions utilizing dual stereo camera systems will also benefit from this method as well.

The effect of subsoil bedrock had a significant effect, as predicted, reducing overall crater diameter and depth (Goulburn and Burnside) when compared to a similar region with loosely packed soil (Hepburn and Sleepy Dragon). The increased thrust loads associated with any possible human Mars mission will naturally intensify the erosion problem. If future vehicles are to use retro-propulsive landing system, it will be important to either choose landing sites with solid foundations or construct a landing site ahead of time.

Volumetric erosion rates agreed well with experimental tests conducted in similar conditions using soil simulants. This agreement validates vacuum chamber testing methodologies for analyzing plume-soil erosion and will allow for better prediction of erosion rates for similar and derived vehicles in the future.

Acknowledgments

The author thanks Cardinal Systems for their excellence in support and expertise and Orrin Thomas of Cardinal Systems for his assistance in creating the geometrical model calibration that was the basis for this analysis.

References

[1]"NASA's Recommendations to Space-Faring Entities: How to Protect and Preserve the Historic and Scientific Value of U.S. Government Lunar Artifacts". National Aeronautics and Space Administration.

[2]Mehta, Manish, et al. Thruster Plume Surface Interactions: Applications for Spacecraft Landings on Planetary Bodies. AIAA Journal 2013 51:12, 2800-2818

[3]Mehta, Manish, et al. "Explosive erosion during the Phoenix landing exposes subsurface water on Mars." Icarus, Volume 211, No. 1, 2011. pp. 172-194.

[4]Hall, L., et al. "Site Alteration, Dust Lifting, and Ground Pressure Study Druing Simulated Mars Science Laboratory (MSL) Landing." 2013.